Orthorhombic to monoclinic phase transition in $NbNiTe_2$

Jennifer Neu,[1] Kaya Wei,[1] Xing He,[2] Olivier Delaire,[2] Ryan Baumbach,[1] Zhenzhen Feng,[3,4,5] Yuhao Fu,[3] Yongsheng Zhang,[4,5] David J. Singh,[3,6] and Theo Siegrist[1,7]

[1]*Condensed Matter Science, National High Magnetic Field Laboratory, Tallahassee, Florida 32312, USA*
[2]*Mechanical Engineering and Materials Science, Duke University, Durham, North Carolina 27708, USA*
[3]*Department of Physics and Astronomy, University of Missouri, Columbia, Missouri 65211-7010, USA*
[4]*Key Laboratory of Materials Physics, Institute of Solid State Physics, Chinese Academy of Sciences, Hefei 230031, China*
[5]*Science Island Branch of the Graduate School, University of Science and Technology of China, Hefei 230026, China*
[6]*Department of Chemistry, University of Missouri, Columbia, Missouri 65211-7010, USA*
[7]*Chemical and Biomedical Engineering, FAMU-FSU College of Engineering, Tallahassee, Florida 32312, USA*

(Received 12 April 2019; published 11 October 2019)

The high-temperature structural phase transition of the potential topological material $NbNiTe_2$ has been studied in detail. At high temperatures, the structure is centrosymmetric with orthorhombic space-group $P\frac{2}{m}\frac{2}{n}\frac{2_1}{a}$ ($Pmna$), and distorts at 373 K to a monoclinic structure with space-group $P11\frac{2_1}{a}$ ($P112_1/a$). A small signature in specific heat and commensurate small release of entropy are observed at the phase transition. The low-temperature monoclinic structure retains its inversion center and the symmetries associated with the orthorhombic c axis. At high temperatures, $NbNiTe_2$ shows phonon instabilities at Γ and X, which are removed by the structural phase transition. The electronic structure of $NbNiTe_2$ is only slightly affected, indicating this ferroic phase transition is primarily due to steric effects.

DOI: 10.1103/PhysRevB.100.144102

I. INTRODUCTION

Phonon-induced structural phase transitions where a phonon mode is temperature dependent are at the heart of a large number of physical phenomena, such as ferroelectricity, ferroelasticity, and ferromagnetism [1]. In systems with strong electron-phonon coupling, a structural transition will affect the electronic band structure and vice versa. In fact, band inversion driven by strong electron-phonon coupling has been proposed as a driving mechanism for topological transitions at finite temperatures [2–6]. The appearance of topological properties upon small distortions are of great importance as they would provide a practical way to switch between trivial and nontrivial topologies using thermodynamic parameters, such as pressure, magnetic field, and temperature.

Previously, Huang *et al.* investigated the compound $NbNiTe_2$ and reported the structure to have space-group $Pm2a$ [7]. Recently, Wang *et al.* found the structure to relax in density functional theory (DFT) calculations to a higher symmetry of $Pmna$, thus indicating that the reported structure is unstable [8]. The atomic displacements leading to the unstable noncentric symmetry $Pm2a$ were found to be accessible by optical phonon modes. The reported phonon band dispersions obtained in the high-symmetry $Pmna$ structure indicate a soft phonon mode that corresponds to a small monoclinic distortion but including finite temperatures and zero-point energy, the $Pmna$ symmetry was deemed to be more stable. Further electronic structure calculations by Wang *et al.* suggest that the lattice distortion to the $Pm2a$ space group results in the emergence of 20 Weyl points [8]. Thus motivated, we synthesized single crystals of $NbNiTe_2$ to further study the potential phase transition and electronic properties.

We find that the samples are metallic and nonmagnetic across the temperature range of 2–400 K. We identify the ferroic structural phase transition resulting in a centrosymmetric monoclinic structure at $T_S = 373 \pm 3$ K. Details of the structural, thermal, and electronic characterizations will be discussed.

II. METHODS

Single crystals of $NbNiTe_2$ were grown by chemical vapor transport, details are given in the Supplemental Material [9]. These crystals were investigated using single-crystal and powder x-ray diffraction (XRD), specific-heat, differential scanning calorimetry, magnetization, and electrical resistivity measurements. Single-crystal x-ray-diffraction experiments with full structure determinations were performed at 200 and 400 K using an Oxford Diffraction Xcalibur-2 CCD diffractometer with graphite monochromatized Mo $K\alpha$ radiation. Both the 200- and the 400-K structure refinements have been deposited as CIFs with the Fachinformationszentrum, Karlsruhe, Germany [10].

Density functional calculations were performed to determine both the electronic and the phononic band structures of $NbNiTe_2$. The phonon calculation and initial relaxation of the structure were performed using the projector augmented-wave method [11] as implemented in the VASP code [12]. The atomic coordinates were then relaxed again using the general potential linearized augmented plane-wave (LAPW) method [13] as implemented in the WIEN2K code [14]. Phonon dispersions were obtained using the finite difference method as implemented in the PHONOPY code [15]. The structure was

relaxed in a scalar relativistic approximation, and spin-orbit coupling was included for the reported electronic structure results.

III. RESULTS AND DISCUSSIONS

$NbNiTe_2$ was originally reported to crystallize in a noncentric orthorhombic structure with the space-group *Pm*2*a* at room temperature [7]. More recently, the related phase $TaNiTe_2$ was reported in the centrosymmetric group *Pmna* [16], thus, raising questions about the exact symmetry in these systems. With an unstable phonon mode driving a transition to the potentially noncentric space-group symmetry *Pm*2*a* and resulting in the emergence of a topologically nontrivial Weyl II semimetal [8], further investigations were warranted. New DFT calculations were performed using the orthorhombic *Pmna* structure as the starting point to elucidate the ground-state structure of $NbNiTe_2$. The calculated phonon dispersions and corresponding phonon density of states of the orthorhombic *Pmna* structure are shown in Fig. 1(I). The instability of an optic branch at the zone center and at the X point are consistent with prior work [8].

In order to computationally characterize the instability, we froze a distortion corresponding to the unstable mode at Γ and allowed for random displacement of the atoms. We then fully relaxed the atomic positions without symmetry imposed, whereas keeping the lattice constants fixed. This relaxation led to a lower-energy monoclinic structure with the space-group $P112_1/a$. The choice of the nonstandard setting for the monoclinic unit cell with a unique c axis is made to retain the order of the unit-cell axes across the different structures. The calculated phonon spectrum for the obtained monoclinic structure shows no unstable phonon branches, and, in particular, we no longer find an instability at the point corresponding to X in the *Pmna* structure. To verify the stability of the monoclinic structure, we further relaxed the atomic positions using the all-electron LAPW method with well-converged basis sets and a dense $12 \times 14 \times 16$ k-point grid for the Brillouin-zone sampling (see Supplemental Material for technical details [9]). Importantly, we find that the ground-state distorted structure is centrosymmetric, retaining the 2_1 axis, inversion center, and glide mirror plane associated with the orthorhombic c axis.

The DFT findings are in excellent agreement with experimental results. Single-crystal XRD studies at 200 K show that, at this temperature, $NbNiTe_2$ is monoclinic with unique axis c with space-group $P112_1/a$ and monoclinic angle $\gamma = 90.77^\circ$. The $NbNiTe_2$ structure remains monoclinic at room temperature as is immediately seen in the splitting of the orthorhombic (211) peak in the powder-diffraction pattern (Fig. 2 inset). Note that this splitting is small and can easily be hidden in heavily ground powder samples. Further low-temperature x-ray powder-diffraction studies in the range of 10–300 K did not give evidence of a structural change. This led us to further investigate $NbNiTe_2$ at higher temperatures.

The structural transition temperature T_S was determined using specific-heat measurements performed on a single crystal of $NbNiTe_2$ (Fig. 3) where a small peak is observed at 373 ± 3 K. Integration of the peak around T_S gives an enthalpy of $\Delta H = 27.4 \pm 0.5$ J/mol of latent heat at the

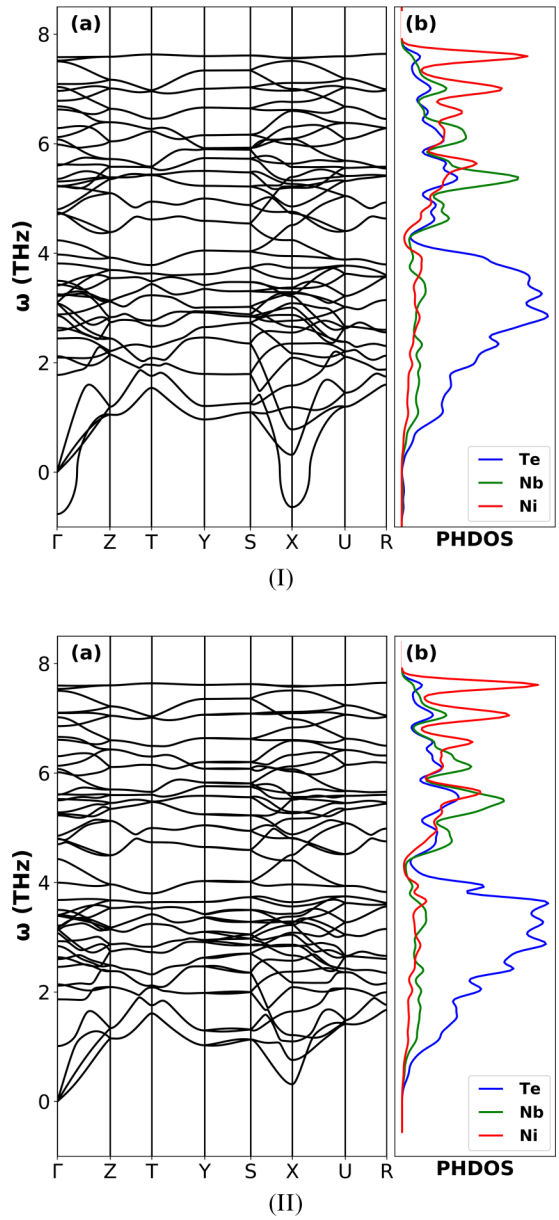

FIG. 1. The phonon spectra for $NbNiTe_2$ in both the orthorhombic *Pmna* (I) and the monoclinic $P112_1/a$ (II) structures are shown above for comparison. (I) Calculated phonon dispersions of $NbNiTe_2$ in the orthorhombic *Pmna* structure. Note the unstable mode at the Γ and X points with imaginary frequencies shown below the horizontal axis. (II) Calculated phonon dispersion of $NbNiTe_2$ in the monoclinic $P112_1/a$ structure. The unstable modes associated with the *Pmna* symmetry have become dynamically stable.

phase transition. The small integrated entropy at the phase transition of $\Delta S = 0.08 \pm 0.01$ J mol^{-1} K^{-1} indicates that the structural phase transition does not substantially modify the configuration space and may be considered as weakly first order. By fitting the data using the Debye function (solid line), we estimate a Debye temperature $\Theta_D = 263$ K, and the low-temperature fit $\frac{C_p}{T} = \gamma + T^2$ gives an electronic coefficient of the heat-capacity $\gamma = 0.0094 \pm 0.0001$ J mol^{-1} K^{-2} (see Supplemental Material Fig. S3 [9]). Differential scanning calorimetry measurements between room temperature

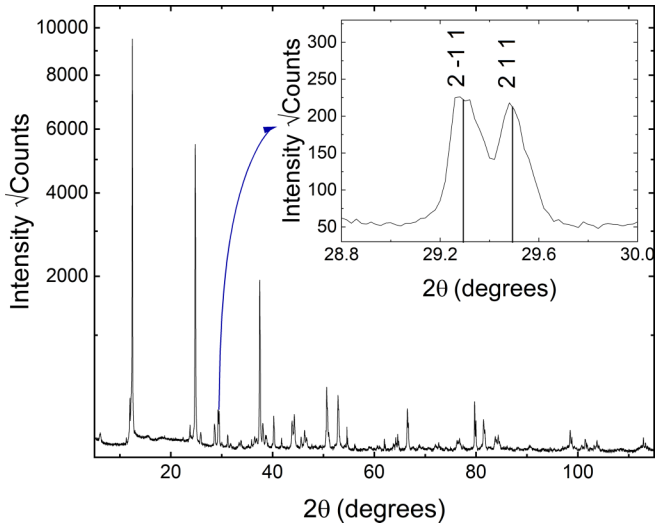

FIG. 2. Splitting of the orthorhombic (211) peak in the powder-diffraction pattern of $NbNiTe_2$ at ambient conditions indicates the symmetry is monoclinic $\gamma \neq 90^\circ$.

and 400 K confirm that the structural transition occurs at a temperature T_S 373 ± 3 K (Supplemental Material Fig. S6 [9]). Additionally, electrical resistivity measurements also show signatures consistent with the phase transition in this temperature range (see Supplemental Material Fig. S4 [9]).

A full structure determination above the phase-transition temperature at 400 K unambiguously shows that the high-temperature phase of $NbNiTe_2$ is orthorhombic with *Pmna* symmetry. Results from single-crystal XRD refinements and DFT structural calculation are shown in Table I. Compared with the lower-temperature phase, the changes in coordinates for all atoms are less than 0.02 Å, indicating that the phase transition does not substantially alter the structure. In the high-temperature *Pmna* structure, the Nb atom is coordinated by four tellurium atoms at short distances, two at 2.789 Å and two at 2.830 Å, plus two tellurium atoms further away at 3.250 Å. Upon the distortion, the long Nb-Te distances are affected most, giving two uneven distances of 3.107 and 3.398 Å (where the mean is 3.253 Å compared to 3.250 Å in the undistorted structure). For the four close Ni-Te distances, the two equal distances in the high-temperature structure at 2.548 Å split into two uneven distances of 2.535 and 2.553 Å (Figs. 4 and 5).

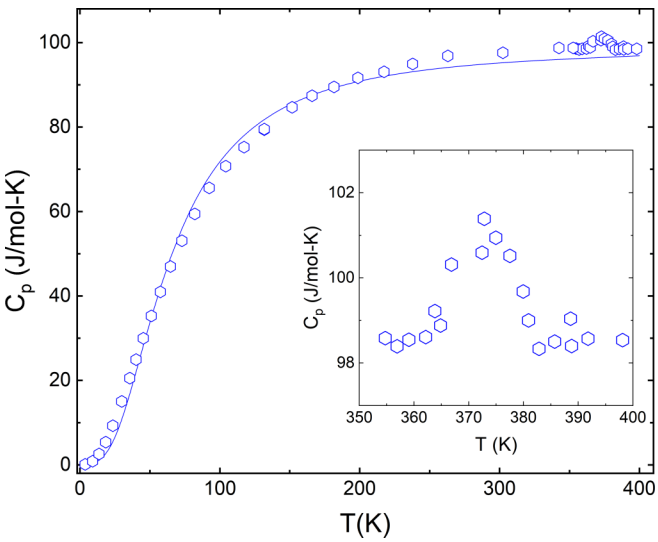

FIG. 3. Single-crystal specific heat of $NbNiTe_2$: $T_S = 373 \pm 3$ K, is shown above. The blue trace is the fitted Debye function. Integration of the peak shown in the inset gives enthalpy of $\Delta H = 27.4 \pm 0.5$-J/mol latent heat about the transition.

TABLE I. *Italicized* lattice parameters were experimentally determined and, subsequently, fixed for DFT calculations. The monoclinic symmetry $P112_1/a$ with a unique c axis is used to emphasize the close relationships to the orthorhombic *Pmna* symmetry.

		$NbNiTe_2$		
		400K XRD	200K XRD	0K DFT
	Spacegroup	53 Pmna	14 $P112_1/a$	14 $P112_1/a$
	a	7.97081(18)Å	7.9572 (19)Å	*7.960197Å*
	b	7.21914(17)Å	7.1991(19)Å	*7.205297Å*
	c	6.27602(13)Å	6.265(16)Å	*6.261397Å*
	γ	90°	90.767(2)°	*90°*
Ni1	Wyckoff	4h	4e	4e
	x	0	0.00115(2)	0.0004
	y	0.1222(2)	0.1221(2)	0.1208
	z	0.14574(19)	0.1458(18)	0.1452
	Uiso[Å²]	0.014	0.009	
Nb2	Wyckoff	4e	4e	4e
	x	0.29464(10)	0.29594(14)	0.2958
	y	0	−0.00955(16)	−0.0108
	z	0	0.00823(12)	0.0088
	Uiso[Å²]	0.014	0.009	
Te3	Wyckoff	4g	4e	4e
	x	0.25	0.25264(9)	0.2501
	y	0.32256(9)	0.32283(11)	0.3248
	z	0.25	0.24824(8)	0.2476
	Uiso[Å²]	0.014	0.008	
Te4	Wyckoff	4h	4e	4e
	x	0	−0.0123(10)	−0.0152
	y	0.22379(9)	0.22442(11)	0.2274
	z	0.75144(9)	0.75165(9)	0.7507
	Uiso[Å²]	0.016	0.009	

The subtle differences in symmetry may be understood using group-subgroup relations. The low-temperature phase $P11\frac{2_1}{a}$ loses the (b-c)-mirror plane present in $P\frac{2}{m}\frac{2}{n}\frac{2_1}{a}$ This loss of a mirror symmetry element and retention of inversion are shown in Fig. 4. The low-temperature phase, up to 373 K is, therefore, a centrosymmetric monoclinic phase with space-group symmetry $P112_1/a$, a subgroup of *Pmna*.

It may be noted that the related systems $NbCoTe_2$ and $TaCoTe_2$ share a similar monoclinic distortion and were also previously classified as orthorhombic. In $NbCoTe_2$ and $TaCoTe_2$, microtwinning masked the small monoclinic distortion, presenting an apparent orthorhombic structure; extensive reinvestigation of these systems eventually led to the correct monoclinic symmetry assignment [17]. We, therefore, believe that similar microtwinning is responsible for the orthorhombic classifications previously assigned to $NbNiTe_2$ at room temperature.

Electronic density functional calculations show that the high-temperature *Pmna* phase is metallic as seen in the

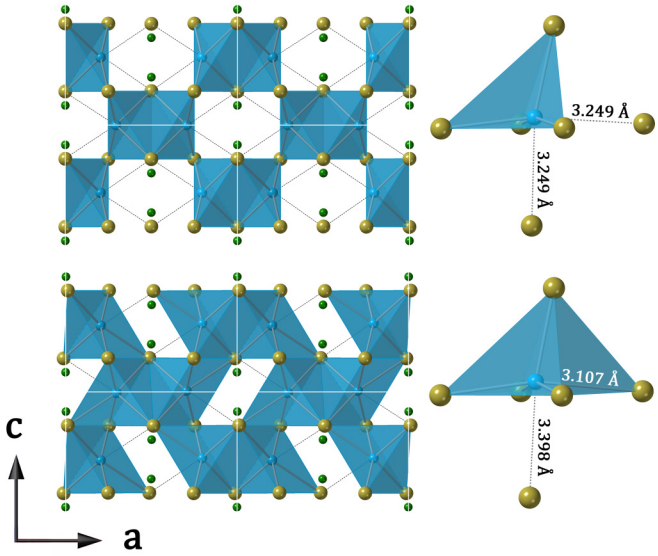

FIG. 4. $NbNiTe_2$ and the associated Nb-Te coordination polyhedra are shown in the high-temperature orthorhombic phase (top) and low-temperature monoclinic phase (bottom).

electronic density of states (DOS) and projections (Fig. 6 and Supplemental Material Fig. S7 [9]). We find little difference between the electronic DOS of the *Pmna* and $P112_1/a$ structures, which is consistent with the observation of metallic behavior across the measured temperature range of 2–400 K (see Supplemental Material Fig. S4 [9]). The structural transition, therefore, does not substantially alter the states at the Fermi level. Unexpectedly, there is even a small increase in the DOS at the Fermi energy ϵ_F after the distortion. Importantly, the Ni *d* shell is nearly full, resulting in a low DOS near ϵ_F (see Supplemental Material Fig. S7 [9]). This is consistent with the fact that $NbNiTe_2$ is nonmagnetic (see Supplemental Material Fig. S5 [9]) and further reduces the driving force for other instabilities driven by the electrons at ϵ_F. We performed additional phonon calculations, similar to those for the orthorhombic phase with the DFT relaxed monoclinic structure. The phonon dispersions show no unstable modes, meaning that this relaxed monoclinic structure is dynamically stable. We also tested the result by performing calculations with the local-density approximation (LDA). We find similar instabilities of the orthorhombic structure with the LDA compared

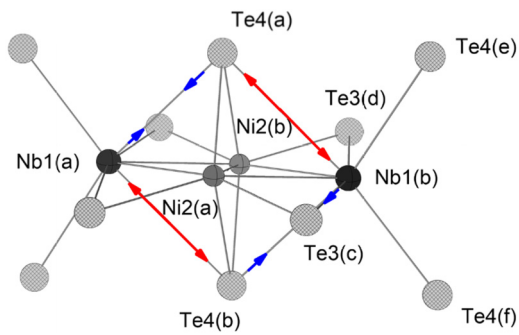

FIG. 5. The primary displacements associated with the low-temperature monoclinic distortion are highlighted. The stretched bonds are indicated with directionally appropriate arrows.

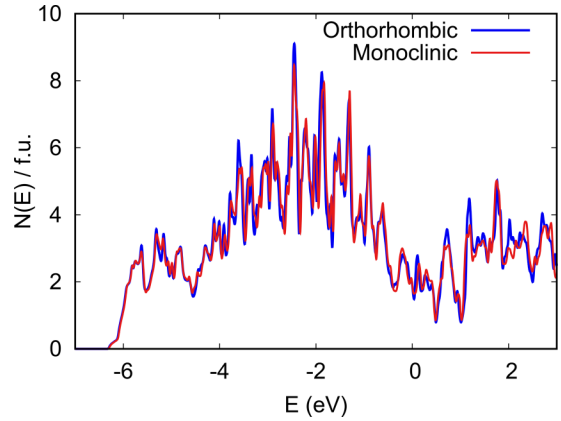

FIG. 6. Total electronic density of states for *Pmna* and $P112_1/a$ $NbNiTe_2$.

to our main results with the Perdew-Burke-Ernzerhof generalized gradient approximation (PBE GGA) functional. The calculated instability energy, including spin-orbit coupling, is 5 meV/f.u. with the PBE GGA functional and 6 meV/f.u. with LDA, respectively.

IV. CONCLUSIONS

To summarize, we find a structure phase transition in $NbNiTe_2$ as confirmed by experimental specific-heat data. The low-temperature structure is monoclinic as found by refinement of x-ray-diffraction data. This structure is in good accord with DFT results, which find an instability of the high-temperature structure. These predict a structure close to experiment for the ground state.

The extremely small changes in the electronic DOS between the two structures signifies that the structural distortion is not a consequence of an electronic instability associated with the band structure near ϵ_F. Rather, the accessible conformations at low temperature are a consequence of the inter- and intralayer nonbonding interactions affecting the phonon spectrum, i.e., sterics. The lowest-energy accessible conformation is realized both computationally and experimentally in the monoclinic $P112_1/a$ structure. The instability in the phonon mode in the vicinity of Γ in the orthorhombic structure *Pmna* is, therefore, the likely driver of the structural distortion without strongly interacting with the electronic system. This structural transition may be classified as ferroic, having changed the point group symmetry of the constituent atoms. However, the ground-state structure of $NbNiTe_2$ remains centrosymmetric and does not host topological electronic states. The small energy differences and atomic displacements between the monoclinic and orthorhombic structures may allow dynamic access to the higher-symmetry orthorhombic structures as, for instance, in pump-probe experiments.

ACKNOWLEDGMENTS

Work at the University of Missouri was supported by the U.S. Department of Energy, Office of Science, Office

of Basic Energy Sciences, Award No. DE-SC0019978. Z.F. is grateful for support from the China Scholarship Council. X.H. and O.D. were supported by the U.S. Department of Energy, Office of Science, Office of Basic Energy Sciences, Award No. DE-SC0019978. J.N. and T.S. acknowledge support from the National Science Foundation under Grant No. NSF/DMR-1606952. K.W. acknowledges support from the NHMFL through the Jack Crow Postdoctoral Fellowship. Part of the work was carried out at the National High Magnetic Field Laboratory, which is supported by the National Science Foundation under Award No. NSF/DMR-1644779 and the State of Florida. Special thanks to V. Glonty and J. Rathfon at Nikon for microscope imaging support. Furthermore, special thanks to T. Figgemeier, a visiting researcher at NHMFL, for his experimental advice and expertise.

[1] E. K. H. Salje, *Phase Transitions in Ferroelastic and Coelastic Crystals* (Cambridge University Press, Cambridge, UK, 1990).

[2] I. Garate, Phonon-Induced Topological Transitions and Crossovers in Dirac Materials, Phys. Rev. Lett. **110**, 046402 (2013).

[3] K. S. and I. Garate, Phonon-induced topological insulation, Phys. Rev. B **89**, 205103 (2014).

[4] B. Monserrat and D. Vanderbilt, Temperature Effects in the Band Structure of Topological Insulators, Phys. Rev. Lett. **117**, 226801 (2016).

[5] G. Antonius and S. G. Louie, Temperature-Induced Topological Phase Transitions: Promoted versus Suppressed Nontrivial Topology, Phys. Rev. Lett. **117**, 246401 (2016).

[6] J. Kim and S. H. Jhi, Topological phase transitions in group IV-VI semiconductors by phonons, Phys. Rev. B **92**, 125142 (2015).

[7] J. L. Huang, S. X. Liu, and B. Q. Huang, Metal-Clusters Synthesized by Solid-State Reaction - Preparation and Crystal-Structure of 2 Mixed Metal-Clusters, $Ni_2Nb_2Te_4$ (I) and $Ni_2Ta_2Te_4$ (II), Science in China Series B-Chemistry Life Sciences & Earth Sciences **34**, 666 (1991).

[8] L.-L. Wang, N. H. Jo, Y. Wu, Q.S. Wu, A. Kaminski, P. C. Canfield, and D. D. Johnson, Phonon-induced topological transition to a type-II Weyl semimetal, Phys. Rev. B **95**, 165114 (2017).

[9] See Supplemental Material at https://link.aps.org/supplemental/10.1103/PhysRevB.100.144102 for $NbNiTe_2$ synthesis details and additional physical property measurement results .

[10] *Inorganic Crystal Structure Database ICSD* (ICSD Nos.: 1897506 and 1897507) (Fachinformationszentrum Karlsruhe, Germany, 2019) https://icsd.fiz-karlsruhe.de/.

[11] G. Kresse and D. Joubert, From ultrasoft pseudopotentials to the projector augmented-wave method, Phys. Rev. B **59**, 1758 (1999).

[12] G. Kresse and J. Furthmüller, Efficient iterative schemes for ab initio total-energy calculations using a plane-wave basis set, Phys. Rev. B **54**, 11169 (1996).

[13] D. J. Singh and L. Nordstrom, *Planewaves, Pseudopotentials, and the LAPW Method* (Springer, New York, 2006).

[14] P. Blaha, K. Schwarz, G. K. H. Madsen, D. Kvasnicka, and J. Luitz, *WIEN2K, An Augmented Plane Wave + Local Orbitals Program for Calculating Crystal Properties* (K. Schwarz, Technische Universität, Wien, Austria, 2001).

[15] A. Togo and I. Tanaka, First principles phonon calculations in materials science, Scr. Mater. **108**, 1 (2015).

[16] W. Tremel, Isolated and Condensed Ta_2Ni_2 Clusters in the Layered Tellurides $Ta_2Ni_2Te_4$ and $Ta_2Ni_3Te_5$, Angew. Chem., Int. Ed. Engl. **30**, 840 (1991).

[17] J. Li, F. McCulley, S. L. McDonnell, N. Masciocchi, D. M. Proserpio, and A. Sironi, X-Ray-Powder Diffraction as a Tool for Facing Twins - the Case of the Monoclinic $NbCoTe_2$ and $TaCoTe_2$ Phases, Inorg. Chem. **32**, 4829 (1993).